catalysts

MDPI

Article

Efficient Removal of Heavy Metals from Aqueous Solutions Using a Bionanocomposite of Eggshell/Ag-Fe

Verónica M. Alamillo-López [1], Víctor Sánchez-Mendieta [2], Oscar F. Olea-Mejía [2], María G. González-Pedroza [1] and Raúl A. Morales-Luckie [2,*]

1 Posgrado en Ciencia de Materiales Facultad de Química, Universidad Autónoma del Estado de, Mexico, Avenida Paseo Colón, esquina paseo Tollocan s/n., Toluca de Lerdo C.P. 50000, Mexico; vmalfq@gmail.com (V.M.A.-L.); marilubell1@hotmail.com (M.G.G.-P.)

2 Centro Conjunto de Investigación en Química Sustentable UAEM-UNAM, Carretera Toluca-Atlacomulco Km 14.5, San Cayetano, Toluca C.P. 50200, Mexico; vsanchezm@uaemex.mx (V.S.-M.); ofoleam@uaemex.mx (O.F.O.-M.)

* Correspondence: ramluckie@gmail.com

Received: 25 May 2020; Accepted: 24 June 2020; Published: 30 June 2020

Abstract: Eggshell and an easily synthesized bionanocomposite of eggshell with Ag-Fe nanoparticles demonstrated to be efficient adsorbent materials for the removal of lead, arsenic, and mercury from water. The natural material and the bionanocomposite were characterized by TEM and XRD. Ag-Fe nanoparticles vary from 1 to 100 nm in size. Equilibrium times of the adsorption systems were achieved between 4 and 8 h. The experimental adsorption data fitted the pseudo-second and Elovich models; therefore, the adsorption of heavy metals ions took place mainly by a chemical process. The adsorption capacity of eggshell in mg/g was 7.01 for As^{5+}, 3.90 for Pb^{2+}, and 1.51 for Hg^{2+}, while the nanocomposite adsorption capacity was 17.7 for As^{5+}, 27.8 for Pb^{2+} and 15.88 for Hg^{2+}.

Keywords: eggshell; silver-iron nanoparticles; adsorption; heavy metals removal

1. Introduction

Heavy metals are one of the most widespread contaminants in water and wastewater [1]. They are toxic and carcinogenic agents. They can be absorbed and accumulated in human body and cause serious health effects like cancer, organ damage, nervous system damage, and in extreme cases, death. The major sources of Pb^{2+} pollution are exhaust gases of petrol engines, which account for nearly 80% of the total Pb^{2+} in the air. Soils located near Pb^{2+} mines may contain up to 0.5% of this metal. Apart from minerals, sources of Pb^{2+} are pesticides, fertilizer impurities, emissions from mining and smelting operations, while atmospheric pollution from the combustion of fossil fuels [2] are generated in electroplating, electrolysis depositions, conversion coating, and anodizing-cleaning, milling, and etching industries from printed circuit board (PCB) manufacturing [1]. Arsenic (As^{5+}) is poisonous and it is used in herbicides, cattle and sheep dips, as desiccant for cotton crop to facilitate the mechanical harvesting of the crop [2], and wood processing [1]. Major contaminating sources of Hg^{2+} are: Hg^{2+} based pesticides, sewage sludge, and atmospheric fall out resulting from the combustion of fossil fuels and industrial processes [2].

On the other hand, egg demand has increased rapidly in past decades; the main egg production is concentrated in 10 countries: China, USA, India, Japan, Mexico, Russia, Brazil, Indonesia, France, and Turkey. Mexico is the number one egg producer in Latin America [3]. The eggshell weighs approximately 10% of the total mass (ca. 60 g) of hen egg, which is transformed into solid waste by food processing and manufacturing plants [4,5]. The hundreds of tons produced every year in

Mexico are causing a strong contamination problem. The chemical composition of eggshell is calcium carbonate (94%), magnesium carbonate (1%), calcium phosphate (1%) and organic matter (4%) [6]. Calcium carbonate is one of the most abundant materials found in sedimentary rock in all parts of the earth surface (it makes up to 4% of the earth's crust). $CaCO_3$ (like calcite) exists in six different forms: three crystalline polymorphs, namely calcite, aragonite, and the metastable vaterite. two hydrated phases (monohydrocalcite $CaCO_3 \cdot H_2O$ and ikaite $CaCO_3 \cdot 6H_2O$), and amorphous calcium carbonate (ACC) [7]. However, by the process known as "biomineralization" it is possible to obtain $CaCO_3$ from eggshell [8]. $CaCO_3$ is stable at atmospheric pressure and temperature, and these minerals affect the chemistry of aquatic systems by regulating pH and alkalinity through dissolution/precipitation equilibrium [9,10]. Moreover, they can govern the mobility and cycling of metal contaminants and radionuclides through ion exchange, adsorption, and co-precipitation reactions [11]. Removal of heavy metals from water has led to numerous investigations mainly because the exposure to them, even at trace levels, is a risk to human health and to ecosystems in general [12]. The adsorption process has come to the forefront as one of the major techniques for heavy metal removal from wastewater. Ahmad et al. [13] used eggshell and coral wastes as low cost sorbents to remove heavy metals Pb^{2+} Cd^{2+} and Cu^{2+}. Pettinato et al. [14] used an eggshell membrane to treat an aqueous solution containing Al^{3+}, Fe^{2+} and Zn^{2+}. Among the available adsorbents, metal oxides (MOs), like iron oxides, are classified as good adsorption materials for heavy metals removal from aqueous systems [15]. The use of metallic oxides has reported good results in the treatment of metals such as lead, arsenic, zinc, nickel and copper [16,17]. Furthermore, metal oxides can combine its magnetic properties with other materials to form composites [15], which can be isolated from water solutions by the application of a magnetic field [18]. Alternatively, silver nanoparticles supported on materials like cellulose [19] or silica [20] have been reported for the adsorption of heavy metals due to their interesting physio-chemical properties, such as, chemical stability, catalytic activity, high adsorption capacity, and their greater dispersion degree [21].

Bimetallic nanomaterials are the combination of two metals at the nanoscale; thus, their performance can be improved because of the metals synergy effects. Usually, the physicochemical properties of bimetallic particles are better than the properties of each metal nanoparticles separately; their structure can be core shell, segregated clusters, nanoalloys or nanoparticles composed of multilayers with alternating layers [22].

A large number of publications and reviews have clearly shown that many types of chemical transformation can be carried out successfully under microwaves (MW) conditions [22–24]. Most importantly, microwave processing frequently leads to a dramatically reduction of reaction times, higher yields, less formation of by-products, easier work-up matching with the goal of green chemistry, solvent-free organic transformations, and selectivity of reactions [25,26]. Microwave-assisted fabrication of nanomaterials can increase the crystallinity of the product. Polar solvents have a good potential to adsorb microwaves and convert them to thermal energy, thus accelerating the reactions, as compared to results obtained using conventional heating [27]. In addition, the synthesized material has a more uniform dimension and composition [28]. Therefore, MW was chosen to synthesize the new composite where the matrix is eggshell and the reinforcement with silver and MO nanoparticles. The first ones favor the formation of iron oxides [29] and the second ones give the material magnetic properties that will help to isolate them after being used as adsorbent material.

Herein, we have designed a nanocomposite based on eggshell and nanoparticles of zero valent silver (Ag^0) and iron oxides (Fe), to enhance the adsorption capability of eggshell for heavy metals in aqueous solution. Moreover, eggshell and its nanocomposite were characterized by Transmission Electron Microscopy (TEM) and X-ray diffraction (XRD). Adsorption kinetics and isotherms studies were performed to understand the plausible mechanisms of removal of ions Pb^{2+}, As^{5+} and Hg^{2+} from aqueous solutions using eggshell and the nanocomposite.

2. Material and Methods

2.1. Eggshell Preparation

Eggshell, collected in bakeries, restaurants, and households, was subjected to a washing treatment with distilled water and brushed to remove organic residuals. It was rinsed, dried (at room temperature for 24 h), and crushed in a mortar. A solution of sodium hypochlorite 1.3% was added to the dried material with constant stirring for one hour. After this time, the material was washed and dried at 50 °C for 24 h. A second grounding process was carried out, this time by a mechanical mill GE motors. By using a stainless-steel sieve set, between 20 and 59 mesh, a fraction of particles was isolated (Mesh 39 ± 1, particles around 0.14 ± 0.008 mm).

2.2. Synthesis of the Nanocomposite [Eggshell/Ag-Fe]

The synthesis of the bionanocomposite was through a redox reaction, where the presence of an oxidizing agent and a reducing agent is necessary as described below. 1 g of dried Eggshell was immersed in 5 mL of aqueous solution of $AgNO_3$ (ACS reagent, =99.0% from Sigma Aldrich) and 10 M $FeSO_4{\cdot}7H_2O$ (ACS reagent, =99.0%) for 1 h, with constant stirring at 200 rpm and room temperature (~25 °C). The mixture was exposed to microwave radiation, for three cycles of 5 min, in a conventional microwave oven, Hamilton Beach brand, model HB-P70B20AP–YU. Afterwards, the bionanocomposite (Eggshell/Ag-Fe) was thoroughly washed with ethanol and deionized water. The synthesized composite was dried overnight at 50 °C to evaporate the solvent.

2.3. Characterization of Eggshell and [Eggshell/Ag-Fe]

2.3.1. Transmission Electron Microscopy (TEM)

Images were taken with a JEOL-2100 electron microscope operated at 200 kV with a LaB_6 filament, operated with a clear, dark field and selected area diffraction. To remove some nanoparticles from the composite, it was dispersed in a solution of isopropyl alcohol and placed in a sonication bath for 40 min at room temperature.

2.3.2. X-Ray Diffraction (XRD)

The natural material was characterized by a Bruker D8 Germany Powder X-Ray diffraction using Cu–Kα radiation (λ = 1.5418 Å), operated at 40 kV and 30 mA (2θ = 5–50°), scan speed of 8° 2θ per min and scan range 5~80°(2θ) was used for this analysis. The crystalline phase of the eggshell, which is calcium carbonate or calcite ($CaCO_3$) was identified by JCPDS-PDF 05-0586.

2.3.3. Sorption Kinetics

The adsorption of heavy metals was studied by batch experiments at room temperature. 10 mg of adsorption material (Eggshell or [Eggshell/Ag-Fe]) and 20 mL of a solution 10 mg/L of the analyte (Pb^{2+}, As^{5+}, or Hg^{2+}) were in contact and stirring at 200 rpm and room temperature. After a specific time (0.25, 0.5, 1, 2, 4, 6, 8, 12, 16 h) the material was separated by centrifugation. The aqueous portion was analyzed by a Perkin Elmer Analyst 200 atomic absorption spectrometer with deuterium lamp as the bottom corrector and an air-acetylene flame.

$$q_e = (C_o - C_e) \times {}^{V}/_{m} \quad (1)$$

where C_o (mg/L) represents the initial concentration of the analyte in the solution and C_e (mg/L) is the concentration after a specific time of contact. V (L) is the volume of each metal solution and m (g) is the mass of adsorbent.

All kinetic data were analyzed by the following mathematical models: pseudo-first order Equation (2), pseudo-second order Equation (3) [30]. Nonlinear fitting methods were applied by using Origin 8.0 software.

A kinetic model is associated with the term "pseudo" when the concentration of one reactant remains constant, it means that the amount is enough that it appears to have no effect on the reaction rate. However, in adsorption kinetic models, the equation was based on the amount of the analyte adsorbed on the adsorbent material instead of the concentration in the liquid phase [31].

According to the pseudo-first order model proposed by Lagergren [32], adsorption takes place on specific sites and there is no interaction between ions. The energy of adsorption is not dependent on surface coverage. The maximum adsorption capacity corresponds to a saturated monolayer on the adsorbent material surface [33].

$$q_t = q_e\left(1 - e^{-k_1 t}\right) \tag{2}$$

where q_t (mg/g) is the adsorption at time t (h), q_e (mg/g) is the equilibrium adsorption capacity, and k_1 (1/h) the adsorption rate constant of first-order sorption.

Pseudo-second order model was introduced by Ho and McKay [34], it suggests that the process takes place by chemisorption.

$$q_t = \frac{k_2 q_e^2 t}{1 + k_2 q_e t} \tag{3}$$

where k_2 (g/mg·h) is the adsorption rate constant.

Second order model, or Elovich model, is widely applied since it describes processes of chemisorption, assuming that the active sites of the sorbent are heterogeneous and therefore exhibit different energies of activation. The process occurs on localized sites and there is interaction between the analyte ions. The energy of adsorption increases linearly with the surface coverage [33].

$$q_t = \frac{1}{\beta}\ln(\alpha\beta) + \frac{1}{\beta}\ln t \tag{4}$$

where α (mg/g·h) and β (g/mg) are the initial adsorption rate, and the constant related to the extent of surface coverage.

2.3.4. Sorption Isotherms

A series of colloidal solutions in a range of 1 to 5 mg/L of the metals (As^{5+}, Pb^{2+} and Hg^{2+}) were prepared, by submerging 1 mg of eggshells in each one; for getting the equilibrium time, the nanocomposite was kept in 25 mL of solution with constant stirring at 200 rpm. Isotherms where analyzed by four different mathematical models: Langmuir Equation (5), Freundlich Equation (6), Sip Equation (7), and Redlich Peterson Equation (8).

Langmuir model considers a chemical adsorption phenomenon [35]. It also considers a thermodynamically homogeneous surface, where only one molecule can be adsorbed on an active site forming a monolayer [36]. The model determines the maximum adsorption capacity of a species on the surface of a solid.

$$q_e = \frac{q_m K_L C_e}{1 + K_L C_e} \tag{5}$$

where q_e is the amount of adsorbate per gram of adsorbent at equilibrium (mg/g), q_m is the maximum adsorption capacity (mg/g), K_L is the Langmuir isotherm constant (L/mg) and C_e is the adsorbate concentration in solution at equilibrium [36,37].

Freundlich's model assumes that the process takes place in multiple layers on a heterogeneous surface and analyzed the exponential distribution of active sites and their energies [38]. This model represents that the adsorption sites have different affinities; therefore, the positions of higher affinity

are occupied first, and later, the bonding energy decrease logarithmically by increasing the occupation of adsorption sites [36].

$$q_e = K_F C_e^{1/n} \tag{6}$$

where K_F is the Freundlich isotherm constant describing the adsorption density (mg/g), and n is a correction factor but also the index $1/n$ is the measure of intensity [38].

The Sip equation includes the isotherm of Langmuir and the Freundlich isotherms considering that the adsorption process at low adsorbate concentrations predicts the Freundlich isotherm, and the monolayer adsorption capacity of Langmuir isotherm at high concentrations [39]. The Sip model is an empirical isotherm equation often expressed as:

$$q_e = \frac{q_m K_s C_e^{1/n}}{1 + K_s C_e^{1/n}} \tag{7}$$

where q_m is the maximum adsorption capacity (mg/g), K_s is the Sips equilibrium constant (mg/L), and n is the Sips constant. It is assumed that the $1/n$ should be ≤1 [39].

Redlich–Peterson model proposes a hybrid isotherm with characteristics of both Langmuir and Freundlich isotherms. [39] The three parameters equation is an empirical equation described as shown:

$$q_e = \frac{K_R C_e}{1 + a_R C_e^g} \tag{8}$$

where K_R and a_R are Redlich–Peterson constants with the respective units of (L/g) and (mg/L), and g is the Redlich–Peterson exponent (dimensionless) where the value is ≤1. This equation becomes linear at a low surface coverage (g = 0) and reduces to a Langmuir isotherm when g = 1 [39].

3. Results and Discussion

3.1. TEM

Transmission electron microscopy has shown that the iron nanoparticles synthesized can vary from 1 to 100 nm in size (Figure 1a). In most cases excessive borohydride is needed to accelerate the reaction to form nanoparticles, and to stabilize and provide a uniform growth of iron crystals [40]. By incorporating ferrous sulfate into the reaction system, two possibilities may occur: obtaining metallic iron particles or either of the crystalline phases of iron oxide. In Figure 1b the analysis of the interplanar distances of crystalline planes obtained by high resolution transmission electron microscopy indicates the presence of iron oxides because iron is so reactive, and the oxidation process took place as soon as it has contact with air. The presence of silver was confirmed by the diffraction pattern (Figure 1c). Silver can improve the reactivity of iron by changing the electronic properties of its surface [19]. Thus, Ag-Fe nanoparticles were incorporated into the support as can be observed in the TEM images.

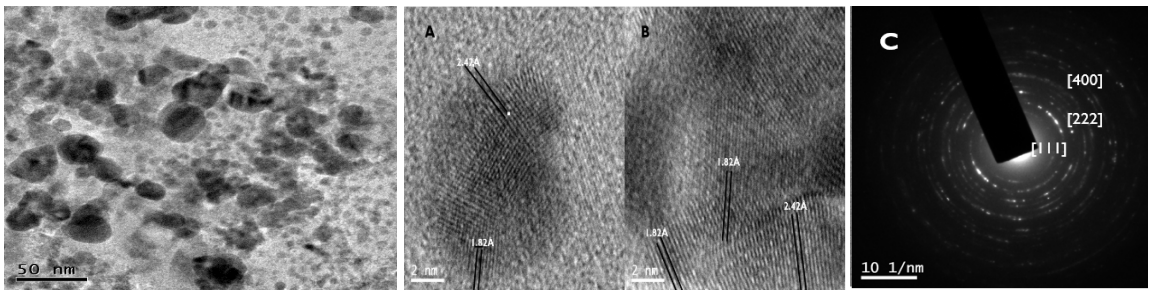

(**a**) (**b**) (**c**)

Figure 1. Micrograph of the composite (**a**), high resolution micrograph of the composite (**b**), and diffraction pattern of the composite (**c**).

3.2. XRD Analysis

The results of XRD for Eggshell are in accordance with those reported for calcite ($CaCO_3$) (Figure 2), implying that this mineral is the major component of the sample, which is also in agreement with previous works [13,41]. The main reflection appeared at 2θ = 29.70 and other peaks at 2θ = 36.30, 39.70, 43.40, 47.30, 47.60, 48.70, 57.60, and 61.60. Those are typical of a rhombohedral structure, hexagonal unit cell, which corresponds to calcite (JCPDS-PDF 05-0586) [42].

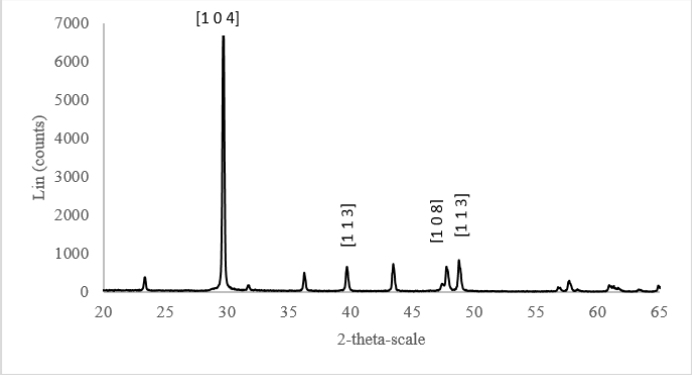

Figure 2. X-ray diffraction (XRD) patterns of eggshell.

3.3. Sorption Kinetics

The contact time is one of the most important factors in the batch sorption process. By this study it is possible to establish the equilibrium time of the process, which means the necessary time for the material to adsorb the analyte to its maximum capacity. In this case, the equilibrium time is established to be applied below in the acquisition of the adsorption isotherms. Moreover, this parameter is important when dealing with practical applications in water treatment processes [43].

Figure 3 illustrates the adsorption kinetic for the adsorption of Pb^{2+}, As^{5+}, and Hg^{2+} with Eggshell and the nanocomposite. Only the best fitted model can be observed in Figure 3; however, the three mathematical models described above were applied, all parameters are presented in Table 1.

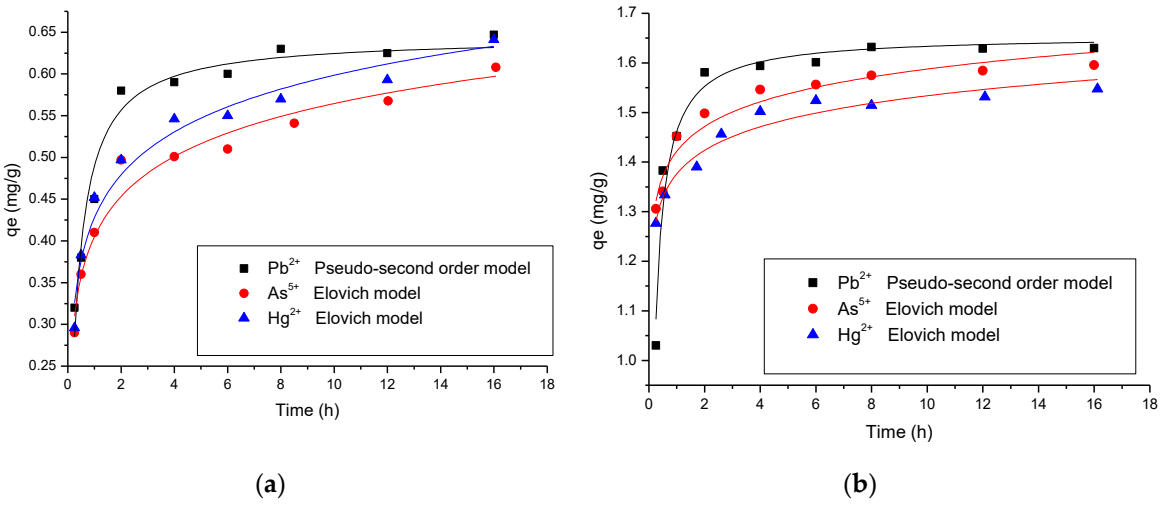

Figure 3. Kinetic of (**a**) Eggshell and the (**b**) nanocomposite for Pb, As, and Hg removal (The symbols represent experimental data while lines are the best-fit mathematical model according to R^2).

Table 1. Values of the characteristic parameters of kinetics models and correlation coefficients for Pb^{2+} As^{5+} and Hg^{2+}.

Adsoprtion Material	Metals	Equilibrium Time (h)	Pseudo-First Order			Pseudo-Second Order			Elovich		
			q_e (mg/g)	k_1 (1/h)	R^2	q_e (mg/g)	k_2 (g/mg·h)	R^2	α	β	R^2
Eggshell	As^{5+}	4	0.532	2.30	0.764	0.565	6.18	0.916	24.17	14.45	0.959
	Pb^{2+}	8	0.601	2.07	0.847	0.637	5.18	0.949	27.3	12.9	0.891
	Hg^{2+}	4	0.562	2.31	0.958	0.599	5.73	0.943	23.78	13.49	0.967
[Eggshell/Ag-Fe]	As^{5+}	4	1.53	6.82	0.515	1.57	10.21	0.895	26.9	13.8	0.945
	Pb^{2+}	4	1.59	4.01	0.936	1.65	4.58	0.964	127.3	8.37	0.738
	Hg^{2+}	4	1.48	7.45	0.804	1.51	11.83	0.804	37.7	14.6	0.955

Experimental data in Supplementary Information Table S1.

The kinetic data, where Eggshell was used as adsorption material, showed that the adsorption process of the three tested heavy metals ions took place in a similar way. During the first two hours of contact, mass transfer may occur until the equilibrium time is established at 8 h for Pb^{2+} removal, where a final plateau was reached at this time. The systems of As^{5+} and Hg^{2+} followed a similar behavior, but the plateau was not so clearly achieved, it seems like these systems increase continuously. However, the equilibrium time was established at 4 h, since from this time, the adsorption is not significant enough to consider that the contact time should increase. The adsorption rates, from the pseudo-second order model, are 5.18, 6.18, and 5.73 (g/mg·h), which correspond to Pb^{2+}, As^{5+}, and Hg^{2+}, respectively; the highest adsorption values correspond to As^{5+} and Hg^{2+}, which reach an equilibrium time faster than the other system. The adsorption of As^{5+} was best described by the Elovich model. Although this model was not the best fit for Pb^{2+}, a comparison of the parameters can be made to obtain more information about the process. The value of the parameter α is higher for Pb^{2+} and β for As^{5+}. This means that, for As^{5+}, the available adsorption surface is greater and that for Pb^{2+} the initial absorption rate is higher.

The pseudo-second order model describes the adsorption of Pb^{2+} onto the natural material Eggshell and onto the composite. Therefore, chemisorption can be considered as the dominant mechanism in both cases. The maximum adsorption capacity was established by the isotherms with the help of the described mathematical models.

3.4. Sorption Isotherms

The adsorption isotherm (Figure 4) represents the relationship between the adsorbed amounts (q_e) and the concentration remaining in the solution (C_e). Isotherm equations are employed to quantify the maximum adsorption capacity of the material and analyzed its interaction with the analyte. For this purpose, different mathematical models can be applied. Each one contains certain constant parameters, which express the surface properties, affinity of the adsorbent and other information to evaluate the adsorption capacity of the adsorbent for metal ions. From the plotted graph, the values of R^2 were obtained to determine which adsorption model better fits the experimental data. Table 2 shows the calculated results of all parameters of Langmuir, Freundlich, Sip, and Redlich–Peterson models for Pb^{2+}, As^{5+}, and Hg^{2+} removal.

The theoretical model of Langmuir is often used to establish the maximum adsorption capacity since this model describes the formation of a monolayer onto the surface of the adsorbent material. According to this model, each adsorption site would be occupied until the maximum adsorption capacity (q_m) of the material is reached. Based on this model, the adsorption capacity of Eggshell is greater for As^{5+} than for Pb^{2+} and Hg^{2+} (7.01 > 3.90 > 1.51 mg/g). Conversely, there is a larger adsorption capacity in the composite regardless of the analyte. In this case, the composite (Eggshell/Ag-Fe) showed a greater adsorption capacity for Pb^{2+} than for Hg^{2+} and As^{5+} (27.8 > 17.7 > 15.88 mg/g).

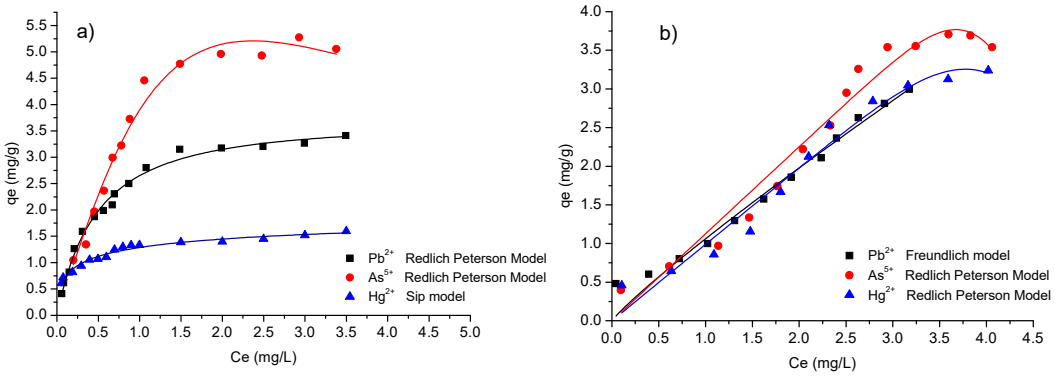

Figure 4. Isotherms of (**a**) Eggshell and the (**b**) nanocomposite for Pb^{2+} As^{5+} and Hg^{2+} removal (The symbols represent experimental data while lines are the best-fit mathematical model according to R^2).

Table 2. Parameters of isotherms model for Pb^{2+} As^{5+} and Hg^{2+} onto Eggshell and composite.

	Parameters	Eggshell			[Eggshell/Ag-Fe]		
		Pb^{2+}	**As^{5+}**	**Hg^{2+}**	**Pb^{2+}**	**As^{5+}**	**Hg^{2+}**
Langmuir	q_m (mg/g)	3.9	7.01	1.51	27.8	17.7	15.88
	K_L (L/mg)	2.07	1.07	7.41	3.83×10^{-2}	7.19×10^{-2}	6.99×10^{-2}
	R_L	0.088	0.157	0.0263	0.839	0.735	0.741
	R^2	0.99	0.932	0.885	0.968	0.935	0.943
Freundlich	1/n	0.365	0.437	0.206	**0.899**	0.875	0.872
	K_F	2.37	3.4	1.25	**1.06**	1.195	1.05
	R^2	0.922	0.844	0.949	**0.97**	0.929	0.939
Sip	q_m (mg/g)	3.87	5.41	**2.16**	112.6	14.54	14.42
	K_S	2.12	2.73	**1.48**	9.42	0.191	0.219
	1/n	0.999	0.518	**0.46**	1.11	0.419	1.503
	R^2	0.989	0.975	**0.97**	0.827	0.955	0.951
* R-P	a_R (L/mg)	**1.84**	**0.256**	27.52	1545.3	**4.07**	**4.83**
	K_R (L/g)	**7.52**	**4.89**	36.4	1641.7	**1.126**	**0.989**
	g	**0.983**	**0.819**	0.848	0.101	**11.3**	**7.77**
	R^2	**0.999**	**0.977**	0.964	0.967	**0.966**	**0.958**

* Redlich-Peterson. Experimental data in Supplementary Information Table S2.

The Langmuir isotherm model can also provide information on whether the adsorption was favorable or unfavorable by the equilibrium parameter or dimensionless constant R_L, which has been disclosed by the following equation:

$$R_L = \frac{1}{1 + K_L C_o} \tag{9}$$

where K_L is the Langmuir constant and C_o is the initial adsorbate concentration (mg/L). While $0 < R_L < 1$ denotes favorable adsorption, $R_L > 1$ is an indication of unfavorable adsorption. R_L values are shown in Table 2, they can be observed in the range of 0.026 and 0.839, which points out that the adsorption process is favorable for all the systems.

All the obtained values of 1/n, from Freundlich model, are between 0.1 and 1 indicating favorable adsorption of Pb^{2+}, As^{5+}, and Hg^{2+} by Eggshell as much as by the composite (Eggshell/Ag-Fe). Although the three isotherm models of Eggshell fit the data well, Redlich–Peterson model exhibited a little better fit for Pb^{2+} and As^{5+}. The same way Sip is the best model for Hg^{2+} isotherm. The value of 1/n from this model is 0.46, which means that the isotherm has a behavior like the Langmuir model. For the bionanocomposite (Eggsell/Ag-Fe), Freundlich model fitted best the experimental data for Pb^{2+} and Redlich–Peterson for Pb^{2+} and As^{5+} since those models exhibit an R^2 value closer to unity. The R^2 value from Freundlich model is close to the value from Redlich–Peterson model; however,

the value of the constants a_R and K_R are above the usual. It means that the model does not present a well adjustment or any that can be considered. The Freundlich model highlights interaction between analyte molecules that leads to the formation of more than one layer on the surface.

In general, the composite showed a higher adsorption capacity to remove any of the three heavy metals tested in the present work compared to the natural material. Table 3 refers to other research focused on the removal by adsorption of these three heavy metals. These studies used other natural materials with and without modifications. The study of Pb^{2+} removal showed that the natural material Eggshell has a lower adsorption capacity compared to other materials, like coral waste and chestnut shell. Eggshell used by Ahmad et al. [13] had an adsorption capacity over 3.9 mg/g. There are some differences between the present work and the one reported by Ahmad, such as particle size and material washing, it is possible that this treatment generates changes in the surface of the material that influences the adsorption process. In that research, the authors pointed out that the main process is ion exchange between the heavy metal ions and Ca^{2+} of the calcite in the eggshell. Also, it is important to consider that eggshell is a natural material which chemical composition can change from one region to another. Coral waste is another natural material proved as adsorption material by Ahmad et al., in this case the capacity is lower (1.14 mg/g). Considering other kind of materials, like nanoscale zero valent iron or bottom ash, the adsorption capacity of our composite [Eggshell/Ag-Fe] is in between the values obtained for those materials (32.8 > 27.8 > 20.0 mg/g).

Table 3. Adsorption capacity of various materials for the removal of lead, mercury, and arsenic.

Reference	Material or Composite	Heavy Metal	Adsorption Capacity (mg/g)
This work	Eggshell-[Eggshell/Ag-Fe]	Pb^{2+}	3.9–27.8
[13]	Eggshell-coral waste	Pb^{2+}	4.7–1.14
[51]	nano-scale zero valent iron	Pb^{2+}	32.8
[52]	Bottom ash	Pb^{2+}	20.0
[53]	Chestnut shell	Pb^{2+}	8.29
This work	Eggshell-[Eggshell/Ag-Fe]	As^{5+}	7.01–17.7
[47]	MIL-53(Fe)	As^{5+}	21.3
[44]	Leonardite char	As^{5+}	8.40
[45]	Biochar sewage sludge	As^{5+}	13.4
[48]	MOF-808	As^{5+}	24.8
This work	Eggshell-[Eggshell/Ag-Fe]	Hg^{2+}	1.51–15.9
[50]	MP-MNa-MC	Hg^{2+}	19.0–23.3–34.8
[54]	Bamboo leaf powder	Hg^{2+}	27.1
[55]	Natural clay	Hg^{2+}	9.70

For As^{5+} removal, the adsorption capacity of the natural material eggshell is close to the value established by Chammui et al. for Leonardite char [44]. Although this value is low compared to the capacities of the other materials described in the table, the composite [EGGSHELL/Ag-Fe] showed a capacity above Biochar sewage sludge proved by Agrafioti et al. [45]. Other materials proved to be better adsorbent materials with greater capacities, like MIL-53(Fe) or MOF-808. However, they need a more complex synthesis method to be developed [46–48].

The adsorption capacity of Eggshell to remove Hg^{2+} is the lowest (1.51 mg/g), but the composite increases its capacity to exceed that reported for other natural materials, such as natural clay [49] and natural mandarin peel (MP) pretreated with NaOH (MNa) [50]. The natural material (Eggshell) has a capacity close to MP. However, the treated MP (MNa—MC) exhibited higher values of 23.3 and

34.8 mg/g, respectively. Another natural material is bamboo leaf powder proposed by Mondal et al. with an adsorption capacity of 27.1 mg/g, although this material was modified with sodium dodecyl sulfate and Triton X-100 solution.

While it is true that some of the materials have a higher adsorption capacity than those studied in this work, their capacity also exceeds to other natural and synthetic materials. Therefore, it is possible to consider the eggshell and its bionanocomposite as potential efficient, low cost, and environmentally friendly adsorbent material.

4. Conclusions

The utilization of eggshell as adsorbent material is an ecofriendly proposition. It is a way of reducing waste and, at the same time, an absorbent material for heavy metals removal from water. Hen eggshell is a material chemically composed by calcium carbonate in the form of calcite. It is a useful material for the removal of lead, arsenic and mercury by a chemical adsorption process onto heterogeneous surface. The adsorption capacity of Eggshell in mg/g was 7.01 for As^{5+}, 3.90 for Pb^{2+}, and 1.51 for Hg^{2+}, while the bionanocomposite [Eggshell/Ag-Fe] capacity was 17.7 for As^{5+}, 27.8 for Pb^{2+}, and 15.88 for Hg^{2+}. Based on correlation coefficient values, the experimental data follows Freundlich, Sip, and Redlich–Peterson isotherms. Adsorption process is favorable for all the systems according to the R_L parameter and the 1/n value from Freundlich equation. Factors such as pH, temperature, adsorbent dose, and particle size should be investigated. Nonetheless, the results from this study provide a better understanding of the adsorption process by a low-cost and renewable material, with the possibility of forming a composite with the bimetallic nanoparticles of silver and iron that increase their potential as an adsorbent material for the removal of heavy metals from water.

Supplementary Materials: The following are available online at http://www.mdpi.com/2073-4344/10/7/727/s1, Table S1. Experimental data of kinetics of Eggshell and the composite for Pb^{2+} As^{5+} and Hg^{2+}; Table S2. Experimental data of isotherms for Pb^{2+} As^{5+} and Hg^{2+} onto Eggshell and composite.

Author Contributions: Experimentation: V.M.A.-L., supervision: R.A.M.-L., Formal analysis: V.S.-M., O.F.O.-M., Review and edition of methodology and proyect administration: M.G.G.-P., conceptualization: R.A.M.-L. All authors have read and agreed to the published version of the manuscript.

Funding: This research received no external funding.

Acknowledgments: V.M.A-L. thanks CONACYT for the scholarship granted to develop this research work.

Conflicts of Interest: The authors declare no conflict of interest.

References

1. Gunatilake, S. Methods of removing heavy metals from industrial wastewater. *Methods* **2015**, *1*, 14.
2. Sherene, T. Mobility and transport of heavy metals in polluted soil environment. *Proc. Biol. Forum Int. J.* **2010**, *2*, 112–121.
3. FAO. Gateway to Poultry Production and Products. Available online: http://www.fao.org/poultry-production-products/products-processing/en/ (accessed on 20 June 2020).
4. Ketta, M.; Tůmová, E. Eggshell structure, measurements, and quality-affecting factors in laying hens: A review. *Czech J. Anim. Sci.* **2016**, *61*, 299–309. [CrossRef]
5. Schott, A.B.S.; Andersson, T. Food waste minimization from a life-cycle perspective. *J. Environ. Manag.* **2015**, *147*, 219–226. [CrossRef]
6. Rodríguez-Navarro, A.B.; Marie, P.; Nys, Y.; Hincke, M.T.; Gautron, J. Amorphous calcium carbonate controls avian eggshell mineralization: A new paradigm for understanding rapid eggshell calcification. *J. Struct. Biol.* **2015**, *190*, 291–303. [CrossRef]
7. Cuesta Mayorga, I.; Astilleros, J.M.; Fernández-Díaz, L. Precipitation of CaCO3 polymorphs from aqueous solutions: The role of pH and sulphate groups. *Minerals* **2019**, *9*, 178. [CrossRef]
8. Villarreal-Lucio, D.; Rivera-Armenta, J.; Martínez-Hernández, A.; Zednik, R.; Moreno, I.E. Effect of nano CaCO3 particles from eggshell on mechanical and thermal properties in pp/eggshell composites. *J. Eng. Technol.* **2018**, *6*, 456–468.

9. Jamil Khan, M.; Zia, M.S.; Qasim, M.S. Contamination of Agro-Ecosystem and Human Health Hazards from Wastewater Used for Irrigation. *J. Chem. Soc. Pakistan* **2010**, *32*, 370–378.
10. Sekkal, W.; Zaoui, A. Nanoscale analysis of the morphology and surface stability of calcium carbonate polymorphs. *Sci. Rep.* **2013**, *3*, 1587. [CrossRef]
11. Caporale, A.G.; Violante, A. Chemical processes affecting the mobility of heavy metals and metalloids in soil environments. *Curr. Pollut. Rep.* **2016**, *2*, 15–27. [CrossRef]
12. Martin, S.; Griswold, W. Human health effects of heavy metals. *Environ. Sci. Technol. Briefs Citiz.* **2009**, *15*, 1–6.
13. Ahmad, M.; Usman, A.R.; Lee, S.S.; Kim, S.-C.; Joo, J.-H.; Yang, J.E.; Ok, Y.S. Eggshell and coral wastes as low cost sorbents for the removal of Pb^{2+}, Cd^{2+} and Cu^{2+} from aqueous solutions. *J. Ind. Eng. Chem.* **2012**, *18*, 198–204. [CrossRef]
14. Pettinato, M.; Chakraborty, S.; Arafat, H.A.; Calabro, V. Eggshell: A green adsorbent for heavy metal removal in an MBR system. *Ecotoxicol. Environ. Saf.* **2015**, *121*, 57–62. [CrossRef]
15. Hua, M.; Zhang, S.; Pan, B.; Zhang, W.; Lv, L.; Zhang, Q. Heavy metal removal from water/wastewater by nanosized metal oxides: A review. *J. Hazard. Mater.* **2012**, *211*, 317–331. [CrossRef]
16. Wang, X.; Guo, Y.; Yang, L.; Han, M.; Zhao, J.; Cheng, X. Nanomaterials as sorbents to remove heavy metal ions in wastewater treatment. *J. Environ. Anal. Toxicol.* **2012**, *2*, 154. [CrossRef]
17. Sharma, S.K. *Heavy Metals in Water: Presence, Removal and Safety*; Royal Society of Chemistry: Jaipur, India, 2014.
18. Yao, Y.; Miao, S.; Liu, S.; Ma, L.P.; Sun, H.; Wang, S. Synthesis, characterization, and adsorption properties of magnetic Fe_3O_4@ graphene nanocomposite. *Chem. Eng. J.* **2012**, *184*, 326–332. [CrossRef]
19. Ali, A.; Mannan, A.; Hussain, I.; Hussain, I.; Zia, M. Effective removal of metal ions from aquous solution by silver and zinc nanoparticles functionalized cellulose: Isotherm, kinetics and statistical supposition of process. *Environ. Nanotechnol. Monit. Manag.* **2017**, *9*. [CrossRef]
20. Ganzagh, M.A.A.; Yousefpour, M.; Taherian, Z. The removal of mercury (II) from water by Ag supported on nanomesoporous silica. *J. Chem. Biol.* **2016**, *9*, 127–142. [CrossRef]
21. Ali, A.; Haq, I.U.; Akhtar, J.; Sher, M.; Ahmed, N.; Zia, M. Synthesis of Ag-NPs impregnated cellulose composite material: Its possible role in wound healing and photocatalysis. *IET Nanobiotechnol.* **2016**, *11*, 477–484. [CrossRef]
22. Vadahanambi, S.; Jung, J.-H.; Oh, I.-K. Microwave syntheses of graphene and graphene decorated with metal nanoparticles. *Carbon* **2011**, *49*, 4449–4457. [CrossRef]
23. Araújo, V.; Avansi, W.; de Carvalho, H.B.; Moreira, M.; Longo, E.; Ribeiro, C.; Bernardi, M.I.B. CeO_2 nanoparticles synthesized by a microwave-assisted hydrothermal method: evolution from nanospheres to nanorods. *CrystEngComm* **2012**, *14*, 1150–1154.
24. Horikoshi, S.; Serpone, N. *Microwaves in Nanoparticle Synthesis: Fundamentals and Applications*; John Wiley & Sons: Weinheim, Alemania, 2013.
25. Ravichandran, S.; Karthikeyan, E. Microwave synthesis-a potential tool for green chemistry. *Int. J. Chem. Tech. Res.* **2011**, *3*, 466–470.
26. Surati, M.A.; Jauhari, S.; Desai, K. A brief review: Microwave assisted organic reaction. *Arch. Appl. Sci. Res.* **2012**, *4*, 645–661.
27. Bilecka, I.; Niederberger, M. Microwave chemistry for inorganic nanomaterials synthesis. *Nanoscale* **2010**, *2*, 1358–1374. [CrossRef]
28. Menéndez, J.; Arenillas, A.; Fidalgo, B.; Fernández, Y.; Zubizarreta, L.; Calvo, E.G.; Bermúdez, J.M. Microwave heating processes involving carbon materials. *Fuel Process. Technol.* **2010**, *91*, 1–8. [CrossRef]
29. Gallo, A.; Bianco, C.; Tosco, T.; Tiraferri, A.; Sethi, R. Synthesis of eco-compatible bimetallic silver/iron nanoparticles for water remediation and reactivity assessment on bromophenol blue. *J. Clean. Prod.* **2019**, *211*, 1367–1374. [CrossRef]
30. El-Khaiary, M.I.; Malash, G.F.; Ho, Y.-S. On the use of linearized pseudo-second-order kinetic equations for modeling adsorption systems. *Desalination* **2010**, *257*, 93–101. [CrossRef]
31. Xiao, Y.; Azaiez, J.; Hill, J.M. Erroneous application of pseudo-second-order adsorption kinetics model: Ignored assumptions and spurious correlations. *Ind. Eng. Chem. Res.* **2018**, *57*, 2705–2709. [CrossRef]
32. Lagergren, S. Zur theorie der sogenannten adsorption gelöster stoffe. *K. Sven. Vetensk. Handl.* **1898**, *24*, 1–39.
33. Largitte, L.; Pasquier, R. A review of the kinetics adsorption models and their application to the adsorption of lead by an activated carbon. *Chem. Eng. Res. Des.* **2016**, *109*, 495–504. [CrossRef]

34. Ho, Y.S.; McKay, G. Pseudo-second order model for sorption processes. *Process Biochem.* **1999**, *34*, 451–465. [CrossRef]
35. Liu, Y.; Liu, Y.-J. Biosorption isotherms, kinetics and thermodynamics. *Sep. Purif. Technol.* **2008**, *61*, 229–242. [CrossRef]
36. Choi, J.; Chung, J.; Lee, W.; Kim, J.-O. Phosphorous adsorption on synthesized magnetite in wastewater. *J. Ind. Eng. Chem.* **2016**, *34*, 198–203. [CrossRef]
37. Langmuir, I. The constitution and fundamental properties of solids and liquids. Part I. Solids. *J. Am. Chem. Soc.* **1916**, *38*, 2221–2295. [CrossRef]
38. Bergmann, C.P.; Machado, F.M. *Carbon Nanomaterials as Adsorbents for Environmental and Biological Applications*; Springer: Berlin/Heidelberg, Germany, 2015.
39. Sogut, E.G.; Caliskana, N. Isotherm and kinetic studies of Pb (II) adsorption on raw and modified diatomite by using non-linear regression method. *Fresenius Environ. Bull.* **2017**, *26*, 2720–2728.
40. Mavani, K.; Shah, M. Synthesis of silver nanoparticles by using sodium borohydride as a reducing agent. *Int. J. Eng. Res. Technol.* **2013**, *2*, 1–5.
41. Zaman, T.; Mostari, M.; Mahmood, M.A.A.; Rahman, M.S. Evolution and characterization of eggshell as a potential candidate of raw material. *Cerâmica* **2018**, *64*, 236–241. [CrossRef]
42. Freire, M.; Holanda, J. Characterization of avian eggshell waste aiming its use in a ceramic wall tile paste. *Cerâmica* **2006**, *52*, 240–244. [CrossRef]
43. Mahmoud, M.E.; Kana, M.T.A.; Hendy, A.A. Synthesis and implementation of nano-chitosan and its acetophenone derivative for enhanced removal of metals. *Int. J. Biol. Macromol.* **2015**, *81*, 672–680. [CrossRef]
44. Chammui, Y.; Sooksamiti, P.; Naksata, W.; Thiansem, S.; Arqueropanyo, O.-A. Removal of arsenic from aqueous solution by adsorption on Leonardite. *Chem. Eng. J.* **2014**, *240*, 202–210. [CrossRef]
45. Agrafioti, E.; Kalderis, D.; Diamadopoulos, E. Arsenic and chromium removal from water using biochars derived from rice husk, organic solid wastes and sewage sludge. *J. Environ. Manag.* **2014**, *133*, 309–314. [CrossRef] [PubMed]
46. Li, J.; Wang, X.; Zhao, G.; Chen, C.; Chai, Z.; Alsaedi, A.; Hayat, T.; Wang, X. Metal–organic framework-based materials: Superior adsorbents for the capture of toxic and radioactive metal ions. *Chem. Soc. Rev.* **2018**, *47*, 2322–2356. [CrossRef] [PubMed]
47. Vu, T.A.; Le, G.H.; Dao, C.D.; Dang, L.Q.; Nguyen, K.T.; Nguyen, Q.K.; Dang, P.T.; Tran, H.T.; Duong, Q.T.; Nguyen, T.V. Arsenic removal from aqueous solutions by adsorption using novel MIL-53 (Fe) as a highly efficient adsorbent. *RSC Adv.* **2015**, *5*, 5261–5268. [CrossRef]
48. Li, Z.-Q.; Yang, J.-C.; Sui, K.-W.; Yin, N. Facile synthesis of metal-organic framework MOF-808 for arsenic removal. *Mater. Lett.* **2015**, *160*, 412–414. [CrossRef]
49. Eloussaief, M.; Benzina, M. Efficiency of natural and acid-activated clays in the removal of Pb (II) from aqueous solutions. *J. Hazard. Mater.* **2010**, *178*, 753–757. [CrossRef]
50. Husein, D.Z. Adsorption and removal of mercury ions from aqueous solution using raw and chemically modified Egyptian mandarin peel. *Desalin. Water Treat.* **2013**, *51*, 6761–6769. [CrossRef]
51. Arancibia-Miranda, N.; Baltazar, S.E.; García, A.; Romero, A.H.; Rubio, M.A.; Altbir, D. Lead removal by nano-scale zero valent iron: Surface analysis and pH effect. *Mater. Res. Bull.* **2014**, *59*, 341–348. [CrossRef]
52. Buema, G.; Cimpeanu, S.M.; Sutiman, D.; Bucur, R.D.; Rusu, L.; Cretescu, I.; Ciocinta, R.C.; Harja, M. Lead removal from aqueous solution by bottom ash. *J. Food Agric. Environ.* **2013**, *11*, 1137–1141.
53. Ertaş, R.; Öztürk, N. Removal of lead from aqueous solutions by using chestnut shell as an adsorbent. *Desalin. Water Treat.* **2013**, *51*, 2903–2908. [CrossRef]
54. Mondal, D.K.; Nandi, B.K.; Purkait, M.K. Removal of mercury (II) from aqueous solution using bamboo leaf powder: Equilibrium, thermodynamic and kinetic studies. *J. Environ. Chem. Eng.* **2013**, *1*, 891–898. [CrossRef]
55. Eloussaief, M.; Sdiri, A.; Benzina, M. Modelling the adsorption of mercury onto natural and aluminium pillared clays. *Environ. Sci. Pollut. Res.* **2013**, *20*, 469–479. [CrossRef] [PubMed]